Later-Stage Spinodal Decomposition in Polymer Solution under High Pressure: Analyses of Scaled Structure Factor†

Junichi Kojima,‡ Mikihito Takenaka,*,§ Yoshiaki Nakayama,‡ and Takeji Hashimoto§

Asahi Kasei Fibers Corporation, Moriyama, Shiga 524-0002, Japan, and Department of Polymer Chemistry, Graduate School of Engineering, Kyoto University, Katsura, Kyoto 615-8510, Japan

Received April 20, 2005; Revised Manuscript Received July 3, 2005

ABSTRACT: Later-stage spinodal decomposition (SD) of polymer solutions (polypropylene/trichlorofluoromethane) after the onset of pressure jump was investigated in situ by using time-resolved light scattering. The time evolution of the scaled structure factor $F(x) \equiv q_m(t,P)^3 I(x)$ with $x \equiv q/q_m(t,P)$ was analyzed as a function of time t at various pressure P's where $q_m(t,P)$ is the magnitude of scattering vector q at maximum scattered intensity at t and P. In the late-stage SD, $F(x)$ becomes universal with time, indicating that the phase-separated structure grows with self-similarity in the late-stage SD. The obtained $F(x)$ was compared with those of other experiments on polymer blends and computer simulations.

I. Background

This work was strongly motivated by an intriguing texture found in nonwoven fabrics produced by a flash spinning[1,2] (a kind of dry-spinning process) of isotactic polypropylene (PP) solution in supercritical liquid of trichlorofluoromethane as a solvent. Figure 1 demonstrates a typical transmission electron micrograph (TEM) obtained on the ultrathin sections of about 50 nm thick, stained with RuO_4 vapor, of the final dry-spun fibers. It showed periodic, more or less continuous network structure of crystalline PP in the air phase. The solidified PP textures are negatively stained on their surfaces, and hence edges of the network-like PP texture appear dark in the TEM image. In the special sample preparation method employed here for the TEM observation, the air phase was replaced by cured epoxy resin in order to avoid a collapse of the porous network structure made out of crystalline PP in the process of ultramicrotoming of the specimens into ultrathin sections. Since epoxy resin is not stained by RuO_4 vapor, the epoxy phase appears bright in the TEM image.

We are excited about basic physical factors giving rise to such nonequilibrium self-assembly as shown in Figure 1 and raise questions why the continuous network-like texture of PP with a considerable periodicity, uniformity in the PP structural entity, and irregular interfaces of PP is formed in the matrix of air phase! The thinnest part of the texture has a thickness about 20 nm which seemingly reflects thickness of isolated lamella-like PP domain orienting nearly perpendicular to the ultrathin section, as schematically shown in part a of Figure 2. The lamella-like domains may be inferred by larger gray textures with an dark edge as shown in the left edge part of Figure 1 which may be a consequence of the inclined orientation of the lamella-like texture of PP with respect to the ultrathin section, as shown in part b of Figure 2. The periodicity of the percolated domains of PP is in submicron scale of ∼0.5

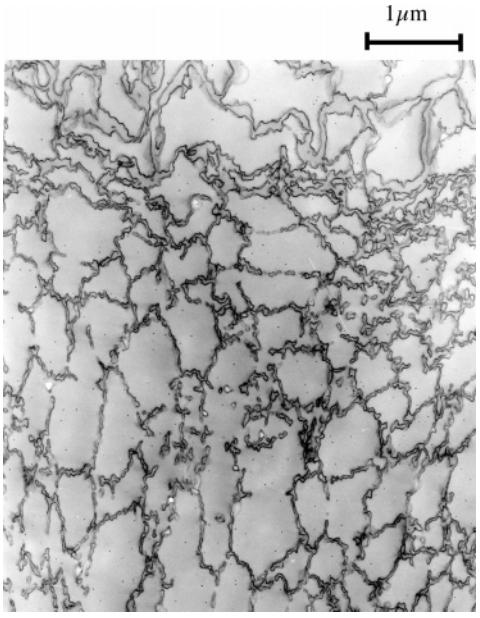

Figure 1. Transmission electron microscope image for flash-spun polypropylene (PP) fibers with PP solution dissolved homogeneously in a supercritical liquid (see text). Ultrathin section stained with RuO_4. The minority phase is the stained PP phase, and the majority phase is the air phase replaced by epoxy resin in order to prepare ultrathin section without damaging the PP network structure.

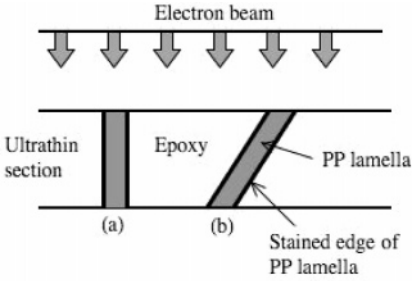

Figure 2. Sketching showing two different orientation of the stained PP lamella in the ultrathin section.

† Presented before; 38th Annual Meeting of the Society of Polymer Science Japan, Yokohama Japan, May 14, 1989, 38th Polymer Symposium of the Society of Polymer Science Japan, Fukui Japan, Oct 3, 1989, and 31st The High-Pressure Conference of Japan, Osaka Japan, Nov 11, 1990.

‡ Asahi Kasei Fibers Corporation.
§ Kyoto University.
* To whom correspondence should be addressed.

10.1021/ma0508350 CCC: $30.25
Published on Web 11/17/2005

μm. The distribution of the dark-to-gray contrast infers the network texture is three-dimensionally continuous. This three-dimensional (3D) network is conceivable from possible ordering processes involved in the flash spinning process also, as will be described below.

We are interested in nonequilibrium path ways which give rise to such intriguing structures. In the experiments yielding the results as shown in Figure 1, a homogeneous solution with 10.5 wt % concentration of PP was first prepared at 215 °C and 14 MPa; the solution was then transferred through a let-down orifice to an enclosure (a let-down zone) controlled at 215 °C and 8.3 MPa for a time period between 0.3 and 5 s. This solution was then spun into fibers through a spinneret of 0.5 mm in diameter with a spinning speed of 11−14 km/min under atmospheric pressure and at an ambient temperature of 30 °C. The fibers had diameters corresponding to 0.1−0.15 denier (g/9000 m) and specific surface area of 20 m^2/g.

The critical pressure above which the solution is homogeneous is 11 MPa at 215 °C. Thus, we anticipate the solution phase-separates at 8.3 MPa (in the let-down zone at 215 °C) where the phase-separated domain structures grow over the time period where the solution was enclosed in the preflush zone.

The growing phase-separated domain structure will be extended by flow and then fixed during the flash spinning process in which the solution was spun through the spinneret and a rapid evaporation of the supercritical solvent occurred. This process involves solidification of PP-rich domains via crystallization, essentially keeping the phase-separated structure unchanged. If the solution is directly ejected under atmospheric pressure and at an ambient temperature of 30 °C without the phase-separation processes in the let-down zone, the obtained products become fluffy and do not form network structures so that the solution cannot be spun into fibers. Thus, only the ejection and the subsequent crystallization cannot form the network structure, and the phase separation in the let-down zone is an important key factor for the formation of the network structure and for flash spinning processes. The intriguing internal structure of spun fibers would reflect liquid−liquid phase separation into polymer-rich phase and solvent-rich phase in the let-down zone and the flow-induced extension during the flash spinning process.

We found[3−5] that the phase separation of this system occurs via spinodal decomposition, which accounts for the observed periodicity of the domain structures. Despite the small volume fraction of PP, PP forms percolated network structures in 3D space, which has been recently clarified due to the stress-diffusion coupling and resulting viscoelastic phase separation process involved in the system having the dynamical asymmetry.[6−9] The percolated domain structures of PP-rich phase are expected to collapse into droplets in much later stage of the phase separation process where the hydrodynamic interactions dominate the domain growth process. However, before the collapse into droplets, the percolated network structures are pinned by vitrification via crystallization induced by the rapid solvent evaporation in process. The roughness of the interface is also a characteristic feature of the viscoelastic phase separation: The local stress are developed in the percolated domains comprised of the entangled PP chains during the domain growth, and the stress relaxation process involves parts of the domain being pulled by another parts of domains, making the interfaces irregular against cost of interfacial tension.

We are interested in whether or not the same shape of domain structure is formed when the flush spinning involves different spinning temperature and pressure and how we can control the internal structure of the flash-spun fibers. This question is reduced to a fundamental question on whether or not the shape of the growing structures developed under different phase separation temperature and/or pressures is universal and how the time evolution of the structure depends on pressure and temperature. Thus, we focus time evolution of scattering structure factors for phase-separating domains as a function of pressure at a given temperature and on universality of the scaled structure factors for the phase-separating domain structures in this work. Even such fundamental studies, aimed for clarification of the self-assembly in the flash spinning process, involves such a challenging experiment that the scattering structure factors occurring in the time scale shorter than about second should be detected in situ and at real time over a sufficiently wide scattering angle.

II. Introduction

In this series of papers,[3−5] we have presented the phase behavior and the spinodal decomposition (SD) of polypropylene solution (PP) in a supercritical fluid of trichlorofluoromethane (CCl_3F). The early-stage SD of PP/CCl_3F was investigated after the onset of pressure jump. The changes in the scattered intensity with time at the early-stage SD can be well approximated by Cahn linearized theory[10] or Cahn−Hilliard−Cook theory.[11] The analyses with the theories yielded the characteristic parameters in the early-stage SD such as the interdiffusion coefficient $D_{app}(P)$ at pressure P and the characteristic magnitude of scattering vector $q_m(0,P)$ at P from the analyses of the time changes in the scattered intensity.

In a companion paper,[5] we investigated the later-stage SD in PP/CCl_3F. The phase-separated structure coarsens with time in the later-stage SD, and the coarsening behavior is characterized by the magnitude of scattering vector $q_m(t,P)$ at maximum scattered intensity and the maximum scattered intensity $I_m(t,P)$ at time t and P. We analyzed the time evolution of $q_m(t,P)$ and $I_m(t,P)$ in order to clarify whether the Langer−Bar-on−Miller (LBM) scaling postulate.[12,13] is valid for the coarsening processes at various P's. As found previously,[14−22] the reduced variables Q_m and $\tilde{I}_m$ plotted as a function of the reduced time τ have been found to become universal with P, where

$$Q_m(\tau) = q_m(\tau,P)/q_m(0,P) \tag{1}$$

$$\tilde{I}_m(\tau) = I_m(\tau,P)q_m{}^3(0,P)/\int_{q''}^{q'} q^2 I(q;\tau,P)\,dq \tag{2}$$

and

$$\tau = t/t_c(P) \tag{3}$$

with q' and q'' being the lower and upper bounds of the wavenumber q, outside of which in the integrand eq 2 becomes effectively zero. q is defined by

$$q = \frac{4\pi}{\lambda}\sin\left(\frac{\theta}{2}\right) \tag{4}$$

with λ and θ being respectively the wavelength of the incident beam and the scattering angle in the medium. Here the characteristic time $t_c(P)$ is given by

$$t_c(P) = [q_m^2(0,P)\, D_{app}(P)]^{-1} \quad (5)$$

In this paper, we shall investigate the later-stage SD of PP/CCl_3F in terms of the scaled structure factor $F(x,t)$ defined by

$$F(x,t) = q_m^3(t,P)\, I(x,t;P) \quad (6)$$

with

$$x = q/q_m(t,P) \quad (7)$$

Previous studies[14,20,23−33] have been reported on the scaled structure factor in the later-stage SD process of phase separation induced by temperature jump. In the intermediate stage, $F(x,t)$ around $x = 1$ was found to increase and sharpen with time, while $F(x,t)$ around $x = 1$ becomes a time-independent universal scaling function $S(x)$, indicating that the global structure of the phase-separated structure grows self-similarly with t. Furthermore, the detail analyses of $F(x,t)$ in the range of x higher than 2 unveiled that $F(x,t)$ at the large x do not still becomes universal in the early time of the late stage, implying that the local structure, such as interfacial structure, cannot be scaled with a single length parameter of $q_m(t,P)^{-1}$. However, in the late time of the late stage, $F(x,t)$ at large x also becomes universal, and the local structure also can be scaled with $q_m(t,P)$. This difference distinguishes the late stage I (early time of the late stage) and II (late time of the late stage).[20,28]

In this paper, we shall check whether the phase-separated structure of PP/CCl_3F grows self-similarly with t in the phase separation induced by pressure jump by investigating the time changes in the scaled structure factor.

III. Experimental Section

Details of the sample and the experimental condition were described in our companion papers.[4] Here we will describe them briefly. The polymer and solvent used here are respectively PP (weight-average molecular weight $M_w = 3.5 \times 10^5$, $M_w/M_n = 6.5$, M_n: number-average molecular weight) and CCl_3F. We used the polymer solution containing 1.5 wt % of the polymer. This concentration is much smaller than the flash spinning experiments described in conjunction with Figures 1 and 2. This concentration is about 10 times the overlap concentration C^* and deliberately set in order to avoid an intense turbidity and multiple scattering effect in the later stage of SD. We quenched the solution from $P = 4.90$ to 4.78 ($\Delta P = 0.1$), 4.73 ($\Delta P = 0.15$), 4.71 ($\Delta P = 0.17$), and 4.67 MPa ($\Delta P = 0.21$), where $\Delta P = P_c - P$ with the cloud point pressure $P_c = 4.88$ MPa at the chosen temperature (432.5 K) of this experiment. It should be noted that the crystallization temperature of bulk at 5 MPa is 403.6 K, which is below the experimental temperature. Thus, the crystallization does not affect the phase separation processes of the polymer solution.

The light scattering instrument used in this study has been shown in our previous papers.[3] We used the photodiode-array light scattering system which enables us to measure the scattered intensity distribution over wide angular range (0°−30° in the air) at 100 scans/s. The changes in the scattered intensity distribution $I(q,t)$ with time after the onset of the pressure jumps were measured by the photodiode-array light scattering system in the q range between 7.4 and 33.2 μm^{-1}. The scattered intensity was corrected for the fluctuation of the incident beam. We also corrected the effects of the turbidity of the sample on the scattered light by using the intensity of the incident beam passing through the sample.[34]

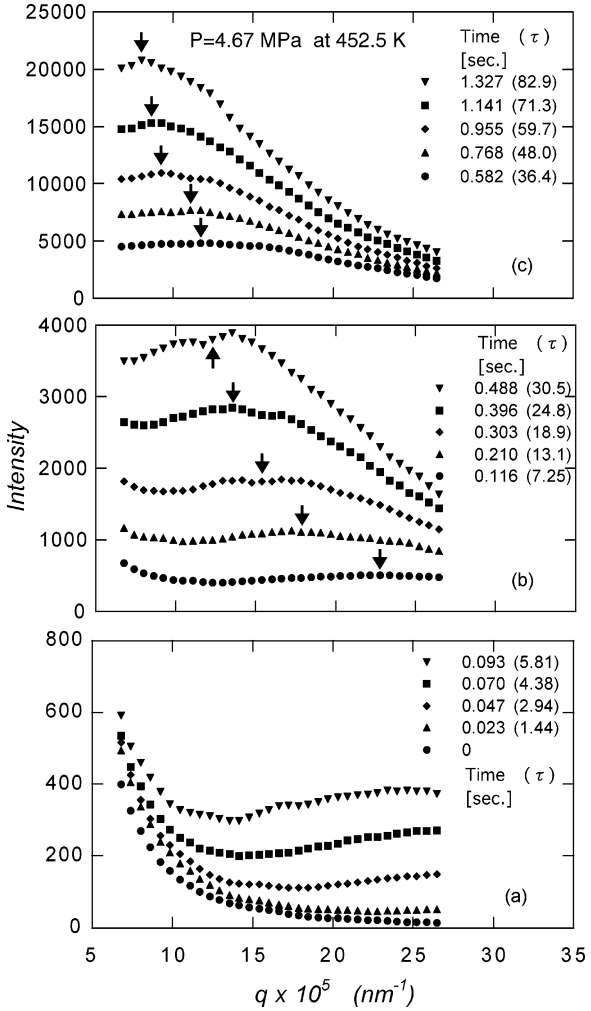

Figure 3. Time change in the scattered intensity $I(q,t)$ plotted as a function of q after the onset of pressure jump from 4.87 to 4.67 MPa at 452.5 K. $P_c = 4.88$ MPa. Time elapses in the order of (a) to (c). The part (a) covers the profiles from 0 to 0.093 s, (b) from 0.116 to 0.488 s, and (c) from 0.582 to 1.327 s after the onset of pressure jump. τ is the reduced time.

IV. Experimental Results

Figure 3 shows the time changes in the scattered intensity after the onset of pressure jump from $P = 4.90$ MPa to $P = 4.67$ MPa at 432.5 K. Here the scattered intensity is plotted as a function of q. Immediately after the pressure jump, the scattered intensity increases with time at the observed q region; subsequently, the peak in the scattered intensity appears at a high q-region. As time elapses, $I_m(t,P)$ increases and $q_m(t,P)$ shifts toward smaller q with t, reflecting the coarsening processes occurs in the later-stage SD.

V. Analyses and Discussion

A. Time Changes in Scaled Structure Factor as a Function of Pressure. Figures 4 and 5 show the time changes in $F(x,t)$ plotted as a function of x for $P = 4.78$ and 4.73 MPa, respectively. In the case of the quenches to $P = 4.78$ and 4.73 MPa, $F(x,t)$ does not become universal with time t during the observed time scale, indicating that the observed coarsening behavior at $P = 4.78$ and 4.73 MPa has not reached the late-stage SD but is still in intermediate-stage SD where the

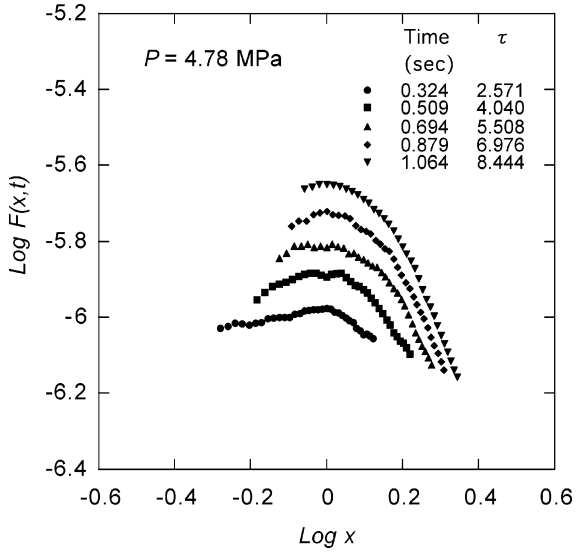

Figure 4. Time changes in $F(x,t)$ plotted as a function of x with t at $P = 4.78$ MPa in double-logarithmic scale. τ indicates the reduced time.

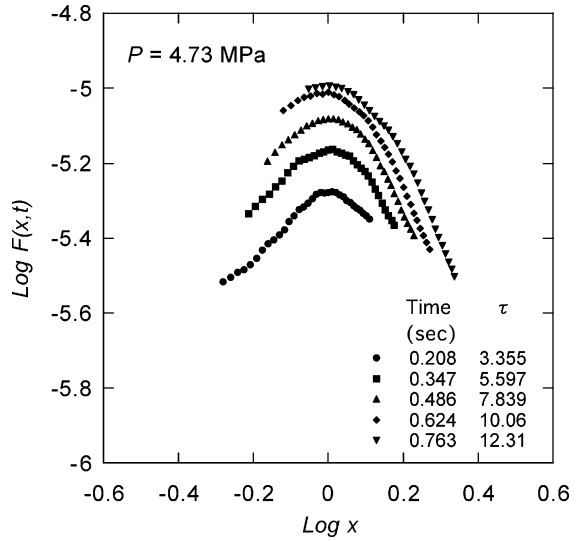

Figure 5. Time changes in $F(x,t)$ plotted as a function of x with t at $P = 4.73$ MPa in double-logarithmic scale.

amplitude of the concentration fluctuation grows with time, and the shape of the domain structure (or more rigorously a spectrum of Fourier models of concentration fluctuations) changes with time. This fact agrees with the fact that the relationship of $\beta > 3\alpha$ was found at $P = 4.78$ and 4.73 MPa, as shown in companion paper,[5] where α and β are the exponents of the power law behavior of $q_m(t,P)$ and $I_m(t,P)$ given by[35]

$$q_m(t,P) \sim t^{-\alpha} \tag{8}$$

and

$$I_m(t,P) \sim t^{\beta} \tag{9}$$

The results shown in Figures 4 and 5 clearly revealed the following pieces of evidence: (i) the phase separation occurs via SD; (ii) a particular Fourier mode with characteristic length $\Lambda_m = 2\pi/q_m$ is selected, and this mode becomes more and more dominant with time; (iii) the growth rate of the mode is obviously larger for the lower pressure with the larger ΔP, giving rise to a larger

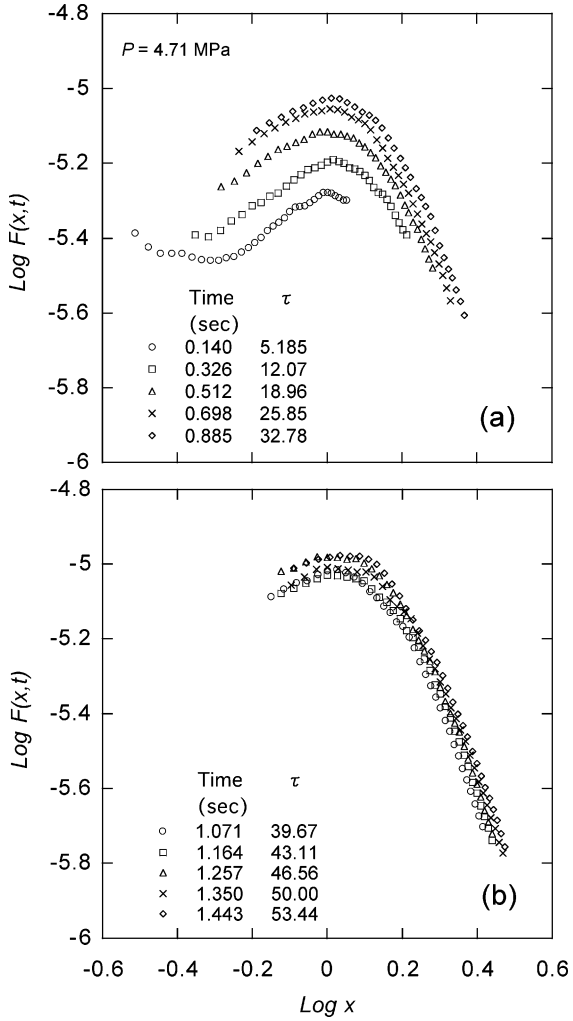

Figure 6. Time changes in $F(x,t)$ plotted as a function of x with t at $P = 4.71$ MPa in double-logarithmic scale: (a) intermediate stage and (b) late stage.

thermodynamic driving force for phase separation. These results elucidate the following characteristic in the time evolution of real-space structure: The systems undergoes SD and, as a consequence, form periodic domains rich in PP solution. The periodicity and identity of domains become clearer with time. It is conceivable that the structure factors shown in Figures 5 and 6 may well present a precursory structure for the final structure developed in the flash-spun fibers shown in Figure 1. Figure 6 shows the time evolution of $F(x,t)$ at $P = 4.71$ MPa. $F(x,t)$ increases with t at $t < 0.885$ s or $\tau < 32.8$ (part a), while $F(x,t)$ becomes almost universal with t at $t > 0.885$ s or $\tau > 32.8$ (part b). The crossover time $t \cong 0.90$ s as observed in the time evolution of $F(x,t)$ agrees with the crossover time from the intermediate-stage to late-stage SD from the change in the relationship between α and β, as clarified previously.[5] The time region $t > 1.071$ s (part b) corresponds to the late-stage SD. The universality in $F(x,t)$ as shown in Figure 6b indicates that the growth of the concentration fluctuations or phase-separated structure satisfies dynamical scaling hypothesis with the single length parameter $q_m^{-1}(t,P)$. Thus, the phase-separated structure of the polymer solution in the late-stage SD grows with the dynamical self-similarity as found for the other systems. Unfortunately, we cannot distinguish the late-stage I from the late stage II and check the existence of the higher order peak at $x = 2$ or 3 as observed previ-

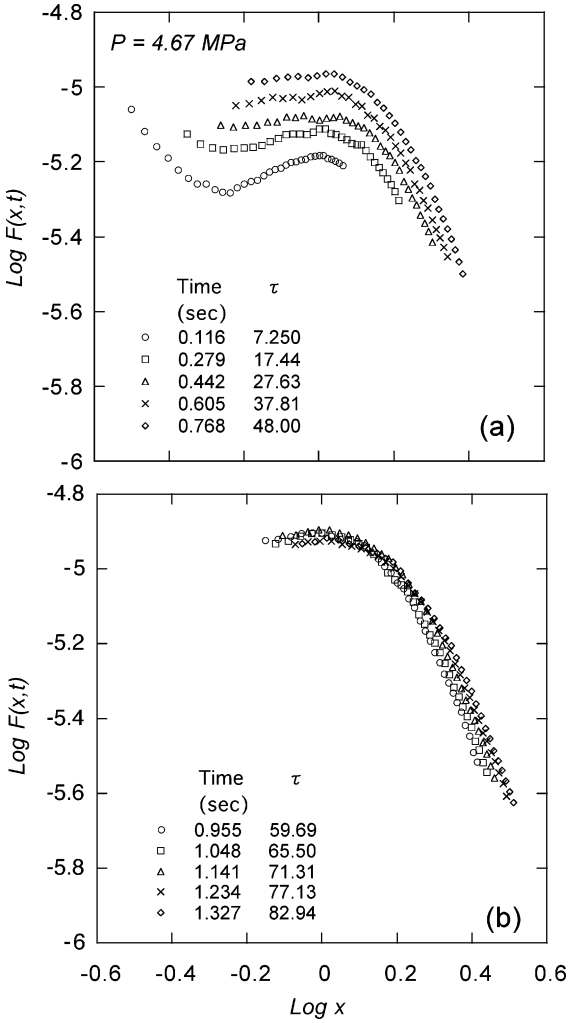

Figure 7. Time changes in $F(x,t)$ plotted as a function of x with t at $P = 4.67$ MPa in double-logarithmic scale: (a) intermediate stage and (b) late stage.

ously,[20,28] since the observed q range is not enough to reach the interfacial region which corresponds to $x > 4$.

The time evolution of $F(x,t)$ at $P = 4.67$ MPa is shown in Figure 7. Similarly to the case of the quench to 4.71 MPa, the crossover from the intermediate stage (part a) to the late stage (part b) is found in $F(x,t)$. The universality in $F(x,t)$ is also found in the late stage at $P = 4.67$ MPa, indicating that the self-similar growth is approximately kept in the late-stage SD at $P = 4.67$ MPa.

Figure 8 presents the pressure dependence of $F(x,t)$ in the late-stage SD. $F(x,t)$ at $P = 4.67$ MPa is slightly broader than that at $P = 4.71$ MPa, showing nonuniversality of $F(x,t)$ with P. This nonuniversality with the quench depth, though in terms of T rather than P, has been found also for polystyrene (PS)/poly(vinyl methyl ether) (PVME),[31] PS/polybutadiene (PB),[24] and polymethylsiloxane (PMES)/ poly(dimethylsiloxane) (PDMS),[32] while the universality with the quench depth (though in terms of T also) has been reported for PB/polyisoprene (PI).[20] This nonuniversality is primarily due to the asymmetry of their phase diagrams, which gives rise to the change in the volume fraction of each phase with the quench depth. This change thus causes the change in the scaled structure factor. On the other hand, the PB/PI system has more symmetric phase diagrams than the other systems, so that the volume fraction of each phase is kept constant.

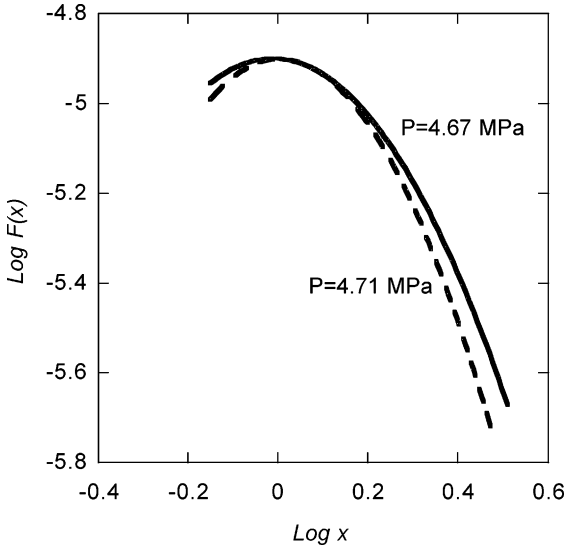

Figure 8. Quench-depth dependence of the universal scaled structure factor $F(x,t)$ in the late stage.

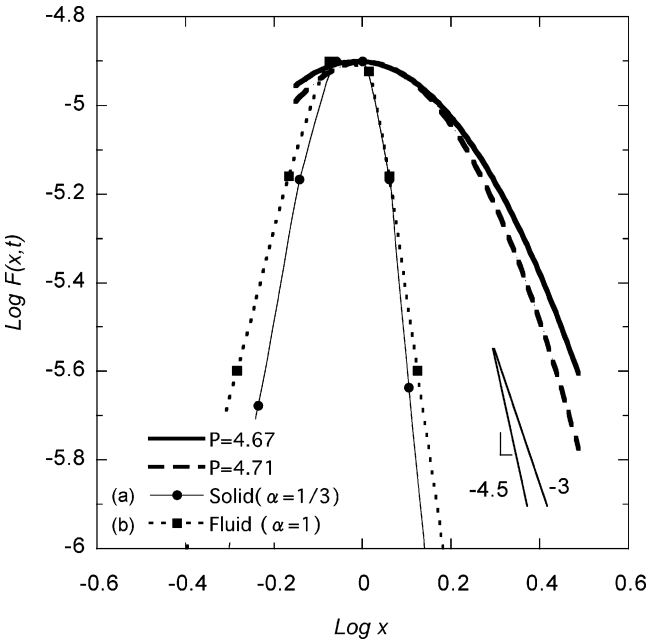

Figure 9. Comparison of our $F(x,t)$ at $P = 4.71$ and 4.67 MPa with those obtained by computer simulations: (a) solid case and (b) fluid case.

B. Comparison of Scaled Structure Factor. Here we compare the universal scaled structure factors obtained in the late-stage SD at $P = 4.71$ and 4.67 MPa, as summarized in Figure 8 based on the results shown in Figures 6 and 7, with those obtained by computer simulations by Koga and Kawasaki[36] in Figure 9. As shown in Figure 9, our scaled structure factors are much broader than those of computer simulations for the fluid case ($\alpha = 1$) where the hydrodynamic interactions play a significant role and the solid case ($\alpha = {}^1/_3$) where the hydrodynamic interactions are completely screened out: the asymptotic behavior of $F(x,t)$ at $x > 1$ is given by $F(x,t) \sim x^{-n}$ with $n \cong 3.0$ over the range of x covered in the experiments and does not agree with $n = 4$ obtained by theory[37] and $n = 4.5$ by computer simulation.[38] This is due to the asymmetry of the volume fraction of each phase in our system, while the theory and computer simulations are based on the symmetric phase diagrams. In our companion paper,[3] we elucidated

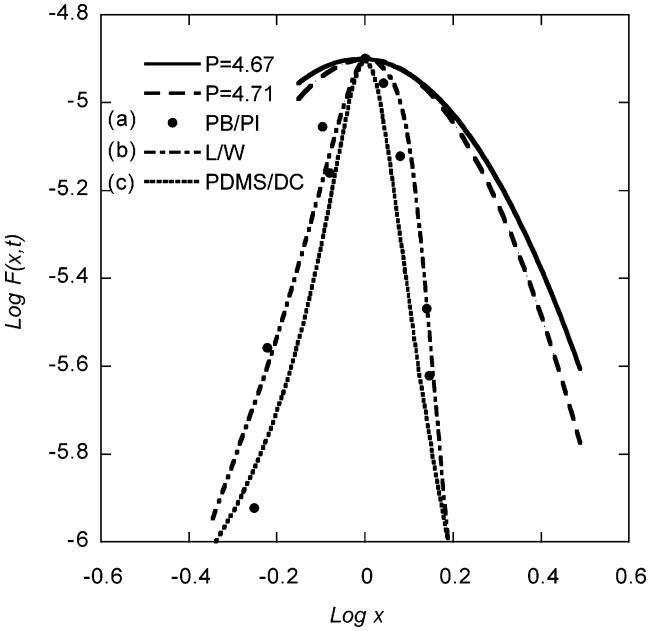

Figure 10. Comparison of our $F(x,t)$ at $P = 4.71$ and 4.67 MPa with those obtained by experiments: (a) PB/PI, (b) L/W, and (c) PDMS/DC.

that the power law behavior of $q_m(t,P) \sim t^{-\alpha}$ at the long time limit in our experiment is given by $\alpha = 0.7$, suggesting the growth mechanism based upon the viscous case in which the hydrodynamic interaction partially, but not fully, becomes important. However, the experimentally observed scaled structure factor reflecting the growth mechanism of the viscous case do not agree with that predicted by the computer simulation based upon the same growth mechanism. This is due to the fact that the exponent α is sensitive to the growth mechanism but insensitive to the asymmetry of the volume fraction. However, the scaled structure factor and hence the shape of the growing domain structure are sensitive to the asymmetry as found for PS/PVME.

Figure 10 shows comparison of our results with the results for the polymer mixture PB/PI[20] and that for small molecular mixture, isobutyric acid and water (L/W).[39] Our results are broader than those of PB/PI and L/W. This difference is caused by the asymmetry of the volume fraction in our system. The scaled structure factors for both PB/PI and L/W were obtained for critical mixtures at shallow quenches and hence for the case where each phase has a symmetric volume fraction.

We also compared our result with that for the polymer solution polydimethlysiloxane/diethyl carbonate (PDMS/DC) by Kuwahara et al.[40] They used monodisperse polymer ($M_w/M_n < 1.02$) while the polydispersity of the PP is relatively wide ($M_w/M_n = 6.5$). The scaled structure factor of PDMS/DC is much sharper than that of our results. This indicates that the polydispersity of polymer may affect the broadening of the scaled structure factor as well as the asymmetry of the volume fraction.

All the results in sections V.A and V.B elucidate that the shape of the growing phase-separated structures is independent of time in the late-stage SD. However, this shape itself sensitively depends on volume fraction of each phase.

VI. Conclusion

Later-stage spinodal decomposition (SD) of polymer solutions (polypropylene/trichlorofluoromethane) after the onset of pressure jump was investigated in situ by using time-resolved light scattering in the time scale shorter than about second and a sufficiently wide scattering angle. The time evolution of the scaled structure factor $F(x) \equiv q_m(t,P)^3 I(x)$ with $x \equiv q/q_m(t,P)$ was analyzed as a function of time t in order to investigate the form of growing domain structures during the isothermal phase-separation process at various pressure P's where $q_m(t,P)$ is the magnitude of scattering vector q at maximum scattered intensity at t and P.

In the case of the two shallower quenches from $P = 4.90$ to $P = 4.78$ ($\Delta P = 0.10$) and 4.73 ($\Delta P = 0.15$) MPa, where $\Delta P = P_c - P$ with the cloud point pressure $P_c = 4.88$ MPa, the scaled structure factor does not become universal with t, since the spinodal decomposition occurs slowly and the coarsening process in the observed time region is still in the intermediate stage of SD, which is consistent with the relationship of $\beta > 3\alpha$ in the observed time region. On the other hand, in the case of the deeper quench to $P = 4.71$ ($\Delta P = 0.17$) and 4.67 ($\Delta P = 0.21$) MPa, we found the universal scaled structure factor in the late-stage SD, indicating that the phase-separated structure grows with self-similarity in the late-stage SD. In other words, the phase-separating structure keeps statistically the same form with time during the phase separation process at a given phase-separation pressure. Only the characteristic length scale of the structure $q_m^{-1}(t,P)$ becomes large with time. The universal structure factor, however, becomes broader with the quench depth ΔP, implying that the scaled structure factor $F(x)$ universal with time is not universal with ΔP.

The universal $F(x)$ was compared with those of other experiments and computer simulations. Our results are broader than those for the other experiments and computer simulations. This difference is caused by the asymmetry of the volume fraction of each phase in our experiment: The other experiments and computer simulations were performed for the case where the volume fraction of each phase is symmetric. The polydispersity also may cause the broadening of the universal $F(x)$.

Thus, the results conclude that a relative volume of each phase sensitively affects the shape of growing phase-separating structure even in the case where the shape is universal with time. Finally, we would like to add a remark associated with the fact that the system is typically dynamically asymmetric one in which mobilities of PP and solvent are drastically different. Thus, phase separation process involves stress−diffusion coupling, and hence the growing domains are subjected to viscoelastic effects. The effects also must affect the scaled structure factors and would make the scaled structure factors less universal with time compared to dynamically symmetric systems. We hope this work gives stimuli for theoretical studies of the viscoelastic effects on the scaled structure factors in future.

Acknowledgment. This work was supported in part by a Grant-in-Aid from Japan Society for the Promotion of Science (15540392 and 14045245).

References and Notes

(1) Andereson, R. D.; Romano, J. E. USP, 3,227,794, 1966.
(2) Blades, H.; White, J. R.; Ford, C. USP, 3,081,519, 1963.
(3) Kojima, J.; Nakayama, Y.; Takenaka, M.; Hashimoto, T. *Rev. Sci. Instrum.* **1995**, *66*, 4066.
(4) Kojima, J.; Takenaka, M.; Nakayama, Y.; Hashimoto, T. *Macromolecules* **1999**, *32*, 1809.
(5) Takenaka, M.; Kojima, J.; Nakayama, Y.; Hashimoto, T. *Polymer* **2005**, *46*, 10782.
(6) Doi, M.; Onuki, A. *J. Phys. II* **1992**, *2*, 1631.
(7) Takenaka, M.; Takeno, H.; Hasegawa, H.; Saito, S.; Hashimoto, T.; Nagao, M. *Phys. Rev. E* **2002**, *65*, 021806.
(8) Tanaka, H. *J. Phys.: Condens. Matter* **2000**, *12*, R207.
(9) Toyoda, N.; Takenaka, M.; Saito, S.; Hashimoto, T. *Polymer* **2001**, *42*, 9193.
(10) Cahn, J. W. *J. Chem. Phys.* **1965**, *42*, 93.
(11) Cook, H. E. *Acta Metall.* **1970**, *18*, 297.
(12) Chou, Y.; Goldburg, W. I. *Phys. Rev. A* **1979**, *20*, 2105.
(13) Langer, J. S.; Bar-on, M.; Miller, H. D. *Phys. Rev. A* **1975**, *11*, 1417.
(14) Hashimoto, T. *Phase Transitions* **1988**, *12*, 47.
(15) Hashimoto, T.; Itakura, M.; Shimidzu, N. *J. Chem. Phys.* **1986**, *85*, 6773.
(16) Inaba, N.; Sato, K.; Suzuki, S.; Hashimoto, T. *Macromolecules* **1986**, *19*, 1690.
(17) Izumitani, T.; Takenaka, M.; Hashimoto, T. *J. Chem. Phys.* **1990**, *92*, 3213.
(18) Kyu, T.; Saldanha, J. M. *Macromolecules* **1988**, *21*, 1021.
(19) Nojima, S.; Shiroshita, K.; Nose, T. *Polym. J.* **1982**, *14*, 289.
(20) Takenaka, M.; Hashimoto, T. *J. Chem. Phys.* **1992**, *96*, 6177.
(21) Takenaka, M.; Izumitani, T.; Hashimoto, T. *J. Chem. Phys.* **1992**, *97*, 6855.
(22) Yang, H.; Shibayama, M.; Stein, R. S.; Shimidzu, N.; Hashimoto, T. *Macromolecules* **1986**, *19*, 1667.
(23) Takenaka, M.; Izumitani, T.; Hashimoto, T. *J. Chem. Phys.* **1990**, *92*, 4566.
(24) Tomlins, P. E.; Higgins, J. S. *J. Chem. Phys.* **1989**, *90*, 6691.
(25) Izumitani, T.; Hashimoto, T. *Macromolecules* **1994**, *27*, 1744.
(26) Hashimoto, T. Ordering Dynamics of Polymer Mixtures at Phase Transition. In *Dynamics of Ordering Processes in Condensed Matter*; Komura, S., Furukawa, H., Eds.; Plenum Publishing Corp.: New York, 1988; p 421.
(27) Hashimoto, T.; Takenaka, M.; Izumitani, T. *Polym. Commun.* **1989**, *30*, 45.
(28) Hashimoto, T.; Takenaka, T.; Jinnai, H. *J. Appl. Crystallogr.* **1991**, 24.
(29) Hashimoto, T. Structure of Polymer Blends. In *Structure and Properties of Polymers*, Thomas, E. L., Ed.; VCH: Weinheim, 1993; p 252.
(30) Hashimoto, T.; Jinnai, H.; Hasegawa, H.; Han, C. C. *Physica A* **1994**, *204*, 261.
(31) Hashimoto, T.; Itakura, M.; Hasegawa, H. *J. Chem. Phys.* **1986**, *85*, 6118.
(32) Nose, T. In *Space-Time Organization in Macromolecular Fluids*; Tanaka, F., Doi, M., Ohta, T., Eds.; Springer: Berlin, 1989; p 40.
(33) Nojima, S.; Ohyama, Y.; Yamaguchi, M.; Nose, T. *Polym. J.* **1982**, *14*, 907.
(34) Stein, R. S.; Keane, J. J. *J. Polym. Sci.* **1955**, *13*, 21.
(35) Gunton, J. D.; Miguel, M. S.; Sahni, P. S. *Phase Transitions* **1983**, *8*, 269.
(36) Koga, T.; Kawasaki, K. *Physica A* **1993**, *196*, 389.
(37) Yeung, C. *Phys. Rev. Lett.* **1988**, *61*, 1135.
(38) Shinozaki, A.; Oono, Y. *Phys. Rev. E* **1993**, *48*, 2622.
(39) Chou, Y. C.; Goldburg, W. I. *Phys. Rev. A* **1980**, *23*, 858.
(40) Kuwahara, N.; Hamano, K.; Aoyama, N.; Nomura, T. *Phys. Rev. A* **1983**, *27*, 1724.

MA0508350